

Retraction Note: Advanced exergy and economic analysis of a hybrid renewable CCHP system for industrial energy and dairy processing

Article Type

Research

Authors

Seyyed Amirreza Abdollahi^{a*}
Seyyed Faramarz Ranjbar^a
Mir Biuok Ehghaghi^a
Moharram Jafari^a

^a Faculty of Mechanical Engineering,
University of Tabriz, Tabriz, Iran

Article history:

Received :30 July 2024

Revised: 18 November 2024

Accepted : 5 December 2024

ABSTRACT

Industrial advancements in recent years have led to a significant increase in global energy consumption. Consequently, the pollution resulting from the use of fossil fuels to meet this energy demand has become a pressing issue. The utilization of biomass as a renewable energy source presents a viable solution to mitigate this problem. In addition to biomass, solar energy has also emerged as a dependable energy source that has been extensively researched in recent times. This study proposes a combined heat and power (CCHP) system that integrates four different systems - biomass, milk powder processing, refrigeration, and photovoltaic panels to generate electricity, milk powder, and cooling capacity. The proposed system underwent optimization through a multi-objective approach to enhance its overall performance and payback period time. The findings indicate that the payback period for the investment can be reduced to 3.82 years, with a maximum cycle efficiency of 33 percent. These values can be adjusted based on the relative importance of each factor. For instance, if the payback period is extended to 4.8 years, the cycle efficiency would decrease to 27 percent.

Keywords: Solar Energy, Biomass, Photovoltaic Panel, Multi-Objective, Optimization.

1. Introduction

The rapid industrial, economic, and societal advancements, coupled with the increasing global population, have led to a surge in energy demand. To address this ever-growing need for energy, there is a reliance on using more and more fossil fuels. However, as fossil fuel reservoirs are finite and expected to be depleted shortly, there is an urgent need to explore and develop new energy sources and systems. Furthermore, the

environmental impacts resulting from the use of fossil fuels, such as irreversible pollution, necessitate a shift towards reducing emissions of pollutants like carbon dioxide, nitrogen oxides, sulfur dioxide, and particles by minimizing the dependency on fossil fuels. [1, 2].

The majority of renewable energy sources stem from solar energy, with the exceptions being geothermal, nuclear, and tidal. In recent years, renewable energy sources have emerged as viable alternatives to fossil fuels. Unlike fossil fuels, these energy sources do not have the same environmental impacts, making them a compelling choice for energy production. Biomass, for example, is a type of fuel that is

* Corresponding author: Seyyed Amirreza Abdollahi
Faculty of Mechanical Engineering, University of Tabriz,
Tabriz, Iran
Email: s.a_abdollahi@yahoo.com

generated through the anaerobic digestion of agricultural, food, forestry, wastewater, and animal waste.[3]

The primary objective of advancing novel techniques in energy systems is to enhance the efficiency of the system, boost production, and minimize the release of harmful pollutants. One promising approach to accomplish this objective is through the implementation of a combined cycle of heat and power (CCHP). These CCHP cycles are highly adaptable and can be employed in various applications with different power ratings. Notably, in recent times, CCHP cycles have found significant utilization in domestic settings. Figure 1 illustrates a CCHP system.

Solar power capabilities are clearly visible, but

the periodic nature and uncertainty of solar energy will impose limitations on this energy source. Consequently, solar energy must be integrated with other energy sources to guarantee a consistent and dependable energy supply.

CCHP Systems can play a crucial role in mitigating the challenges faced by solar energy systems. By utilizing multiple energy sources in conjunction with solar energy, CCHP systems can serve as supplementary sources and contribute to an optimal design for the desired service.

The novelty of the present work is that the system is used to produce milk powder as a side product which is a less common side product in similar cycles. Along with milk powder heat and power is also generated.

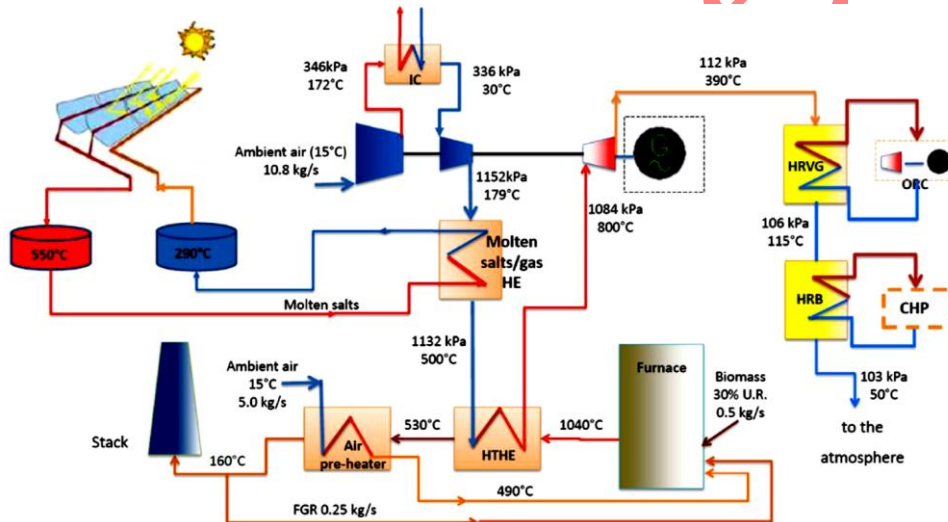


Fig. 1. Biomass-Solar System for Combined Cycle Power Plant [6]

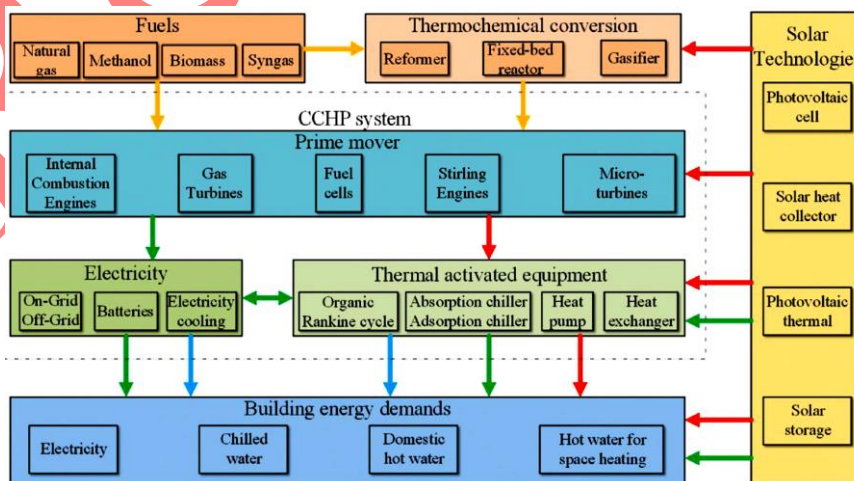


Fig. 2 . Energy Stream For different CCHP Systems of Energy [18]

Nomenclature

\dot{m}	Mass flow rate (kg/s)
Q	Heat transfer (kW)
Z	Exergy-Economic Factor
T_{amb}	Ambient temperature ($^{\circ}\text{C}$ or K)
P	Pressure (bar)
W	Work (kW)
T	Temperature of component ($^{\circ}\text{C}$ or $^{\circ}\text{K}$)
η	Exergy efficiency (%)
Ψ	Exergy efficiency (%)

2. Materials and Methods

The flexibility of CCHP systems utilizing various renewable energy sources allows for their application in both large-scale industrial facilities and small-scale residential setups. This adaptability stands as a significant benefit of these systems compared to others.

Biomass is composed of various gaseous compounds, predominantly Methane, and carbon dioxide. [4] Methane is the primary constituent of biomass. Extensive research has been conducted on biomass in recent years. As indicated by Abdeshahian [5] et al, the electricity generated in Malaysia through Anaerobic digestion of biomass is approximately 8.27 trillion watt-hours.

Various techniques such as pyrolysis,

gasification, and Anaerobic digestion can be utilized for the industrial production of biomass. Anaerobic digestion stands out as a sustainable approach that results in biomass production without generating any byproducts. Additionally, this method requires significantly less space in comparison to alternative methods.

Solar heat collectors (SHC) and photovoltaic panels (PVT) have been used in both industrial and domestic applications. Considering the recent developments, solar systems can play a vital role in CCHP systems. Solar systems can be coupled with other systems like wind and other combined energy systems. Combining such systems can lead to more efficient systems and can be used for many applications such as power, heating and cooling. Solar energy can be stored with energy storage systems and be used in other energy systems. For example, biomass-solar along with the Brayton cycle has been proposed by Pantaleo et al. [6]

PVT panels harness solar energy to generate electricity. These panels come in two variants: silicon crystal and thin film. [7].

Absorption refrigeration cycles are frequently employed for cooling purposes. The cycle requires a heat source to operate effectively. The absorption system can utilize the waste energy from various systems' exhaust streams to provide the necessary heat for the cycle.

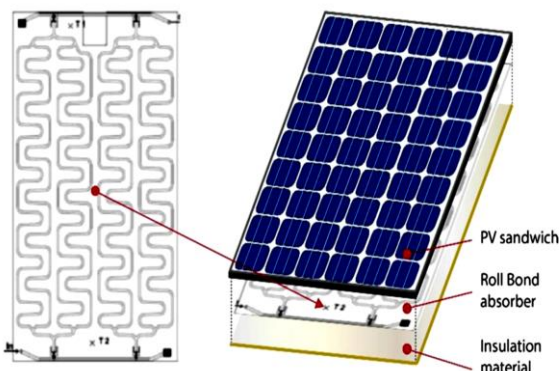


Fig. 3. PVT Panels Structure [9].

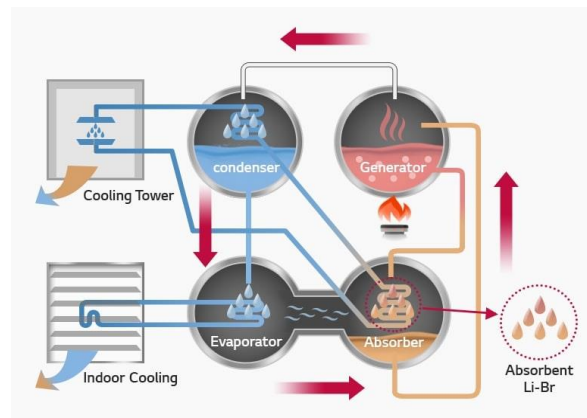


Fig. 4. Schematic of Absorption Refrigeration Cycle

In this paper, a novel approach will be proposed to generate electricity, milk powder, and cooling by utilizing biomass as a fuel source. The process is depicted in Figs. 5 and 6, where the initial step involves the production of biomass through anaerobic digestion, followed by the combustion of biomass and air. The energy released from this combustion process is harnessed in a steam generator, which powers the Rankine cycle (also known as the steam cycle). The steam generated in the Rankine cycle then passes through a steam turbine, where it is converted into electricity using a generator.

It is worth noting that even after the steam generator, the outlet flow still retains energy in the form of heat, which can be effectively utilized. This high-temperature stream is employed in the milk powder production cycle and is transferred to the milk powder cycle through a heater.

Furthermore, to facilitate the production of cooling, an absorption cycle is integrated with the aforementioned process. The heat required for the absorption cycle is supplied by a solar

panel system, ensuring a sustainable and environmentally friendly approach to cooling production.

The equations below represent the conservation of energy and exergy for every component within the system.

$$\dot{Q}_{C.V} - \dot{W}_{C.V} = \sum \dot{m}_{out} h_{out} - \sum \dot{m}_{in} h_{in} \quad (1)$$

$$\dot{E}_D = \sum \dot{E}_{in} - \sum \dot{E}_{out} \quad (2)$$

In Eq.(2), the rate of exergy transfer (\dot{E}) is equivalent to the mass flow rate of exergy ($\dot{m}e$) and is the combination of physical and chemical exergy, where (e) represents the total specific exergy.

$$\bar{e} = \bar{e}^{ph} + \bar{e}^{ch} \quad (3)$$

Equation (4) enables the computation of the precise exergy of the fluid flow in terms of its physical characteristics.

$$\bar{e}^{ph} = \bar{h} - \bar{h}_0 - T_0(\bar{s} - \bar{s}_0) \quad (4)$$

Equation (5) enables the computation of the specific exergy of a chemical substance.

$$\bar{e}^{ch} = \sum_{i=1}^j y_i \bar{e}_i^{ch} + \bar{R}T_0 \sum_{i=1}^n y_i \ln(y_i) \quad (5)$$

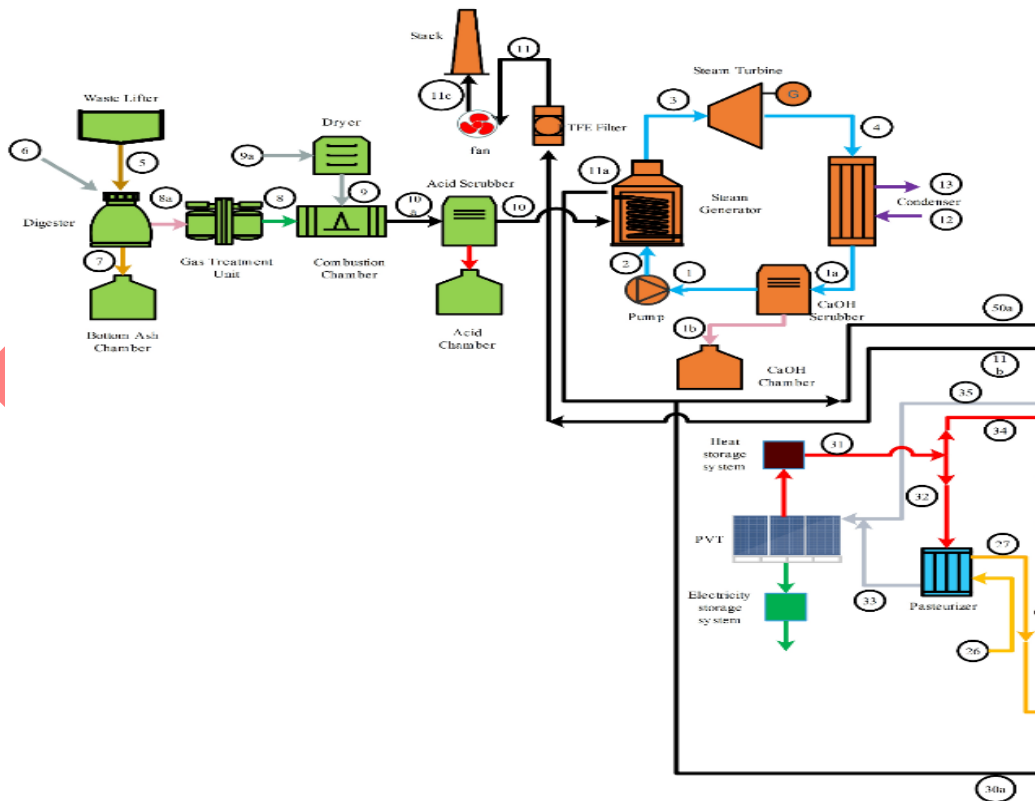


Fig. 5. PVT Panels Structure.

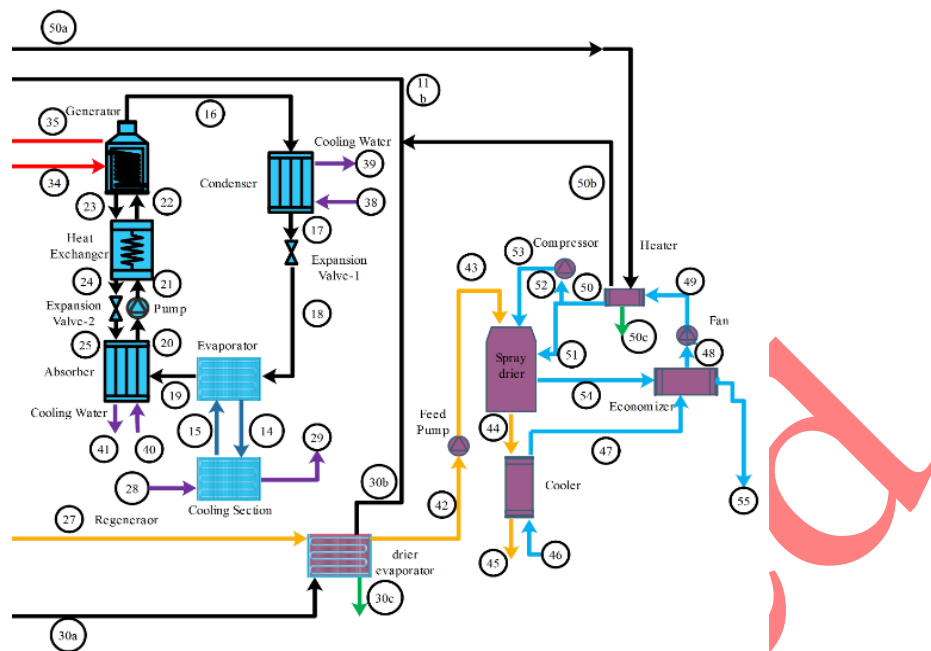
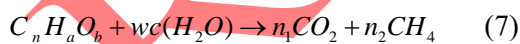


Fig. 6. Cooling and Milk Powder Section of the Proposed Cycle

Equation (5) demonstrates that the rate of exergy destruction is equivalent to the total exergy of the inlet and outlet streams. Exergy efficiency can be determined by utilizing Eq. (6).

$$\varepsilon_i = \frac{\dot{E}_{P,i}}{\dot{E}_{F,i}} \quad (6)$$

During the Anaerobic digestion process, the initial substance undergoes heating to a temperature of 55°C without the presence of oxygen. By applying the technique established by Buswell and Hatfield [8], one can forecast the composition of the resultant biomass gas. In a broad sense, the chemical reaction involved in the generation of biomass through Anaerobic digestion can be described as follows.



In Eq.(7), the subscripts will vary depending on the primary material utilized in the production of biomass.

The Higher heating values for the different types of waste are 16.56, 16.09, and 11.92 MJ/kg, respectively. To determine the chemical

exergy of biomass, the empirical relation provided in Eq. (8) can be employed, considering the non-homogeneous texture of the biomass.

$$e_{manu,daf}^{ch} = \frac{1.044 + 0.016 \frac{z_H}{z_C} + 0.3493 \frac{z_O}{z_C} (1 + 0.0531 \frac{z_H}{z_C})}{1 - 0.4124 \frac{z_O}{z_C}} LHV_{manu,daf} \quad (8)$$

In Eq. (7), Z_H , Z_C , and Z_O are the hydrogen, carbon and oxygen mass fraction in biomass respectively.

Joshi et al [9] presented the mathematical equations necessary for the modeling of the solar panel.

There are several approaches available for exergy-economic Optimization, including Exergy cost theory, Average cost approach, and Specific exergy costing. In this particular investigation, the focus is on Exergy cost. This method involves formulating Eq. (9) for every component within the system.

$$\sum \dot{C}_{out,k} + \dot{C}_{W,k} = \sum \dot{C}_{in,k} + \dot{C}_{Q,k} + \dot{Z}_k \quad (9)$$

Table 1. The Component of Biomass Based on Primary Material Compound.

Type of waste	C	H	O	N
Cow waste	38.06	5.18	28.15	1.85
Sheep waste	37.64	5.06	28.64	1.87
Chicken waste	26.77	3.33	30.52	2.25

Equation (8) represents the relationship between the initial capital cost (C) and the cost of using and maintaining (Z) a particular system. Additionally, $\dot{C}_{w,k}$ and $\dot{C}_{Q,k}$ denotes the cost rate of work and heat, respectively. It is possible to calculate all these parameters by utilizing the equations provided below.

$$\dot{Z}_k = \dot{Z}_k^{CI} + \dot{Z}_k^{OM} \quad (10)$$

$$\dot{C}_{in} = c_{in} \dot{E}_{in} \quad (11)$$

$$\dot{C}_{out} = c_{out} \dot{E}_{out} \quad (12)$$

$$\dot{C}_Q = c_Q \dot{E}_Q \quad (13)$$

$$\dot{C}_W = c_W \dot{E}_W \quad (14)$$

Equation (15) can be employed to compute \dot{Z}_k based on the procurement cost of the equipment.

$$\dot{Z}_k = CRF \times \frac{\phi}{N} \times PEC_k \quad (15)$$

In Eq. (15), CRF, N, and Φ_r denote the cost return factor, annual working hours (assumed as

7880 hours in this study), and maintenance factor (assumed as 1.06 in this study). The exergy-economic equation for each component of the cycle is provided in Table 4. The initial capital costs for each component are listed in Table 6. [10-13]

3. Results and Discussion

Firstly, this section will delve into the topic of validation, followed by an examination of the outcomes derived from the modeling and optimization of the cycle.

Wellinger's work [14] is being compared with the current study to validate the findings on biomass production.

The study of Behzadi et al [12] was consulted for validating the outcomes of the biomass and Rankine sub-system. A visual representation of the comparison of the results can be observed in Fig. 7.

Table 2. Validation for Biomass Production Cycle [14]

Chemical Component	Current work	Reference Work [14]
CH ₄ (%)	58.4	58
CO ₂ (%)	41.6	42

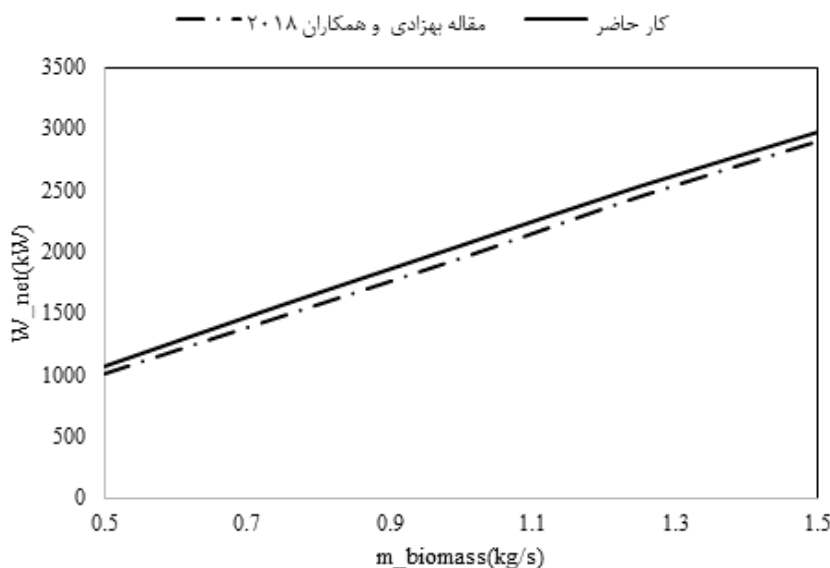


Fig. 7. Validation of Biomass and Rankine Cycle [12].

Aman's work [15] will be cited in Fig. 8 to confirm the findings of the absorption refrigeration cycle.

The rate of exergy destruction for each component which is calculated in the present

work and comparison with reference work are provided in Table 3. In this section, since Multi-objective optimization will be conducted both parameters of the payback period and exergy efficiency will be optimized simultaneously.

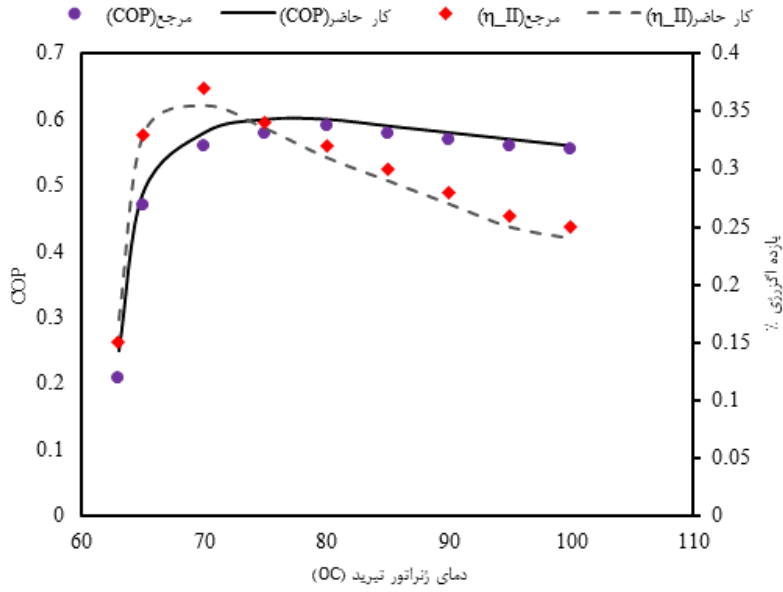


Fig. 8. Validation of Absorption Refrigeration Cycle.

Table 3. exergy destruction rate for the main component of the cycle [16]

Aim	Payback period	Exergy efficiency (%)	Biomass mass flow rate (kg/s)	Milk powder mass flow rate (kg/s)	Solar Panel surface Area (m ²)	Cooling Capacity (kW)	Combustion Chamber inlet Temperature (°C)	Turbine inlet pressure (kPa)
Payback period	3.82	24.7	1.61	2.94	570	20	1185	2200
Optimum exergy	12.5	33	0.7	2.7	440	180	1400	2500

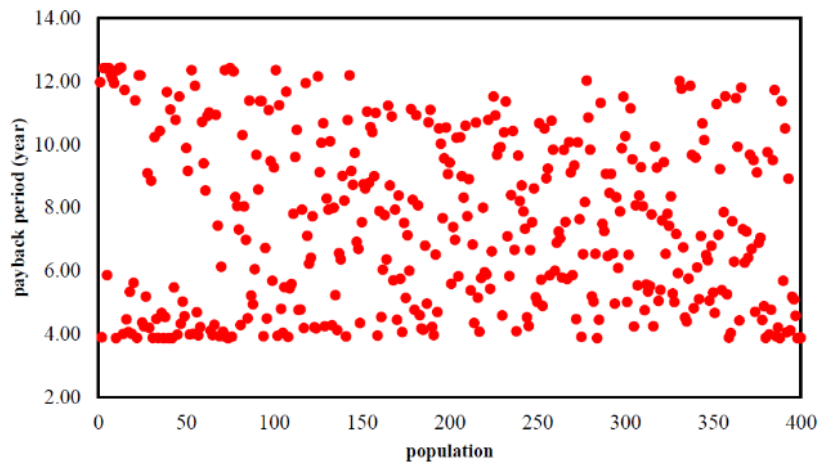


Fig. 9. Results of Multi-Objective Optimization of Payback Period.

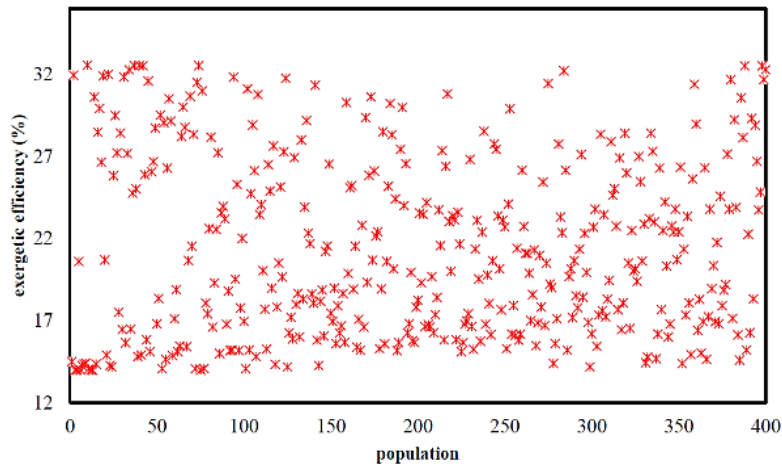


Fig. 10. Results of Multi-Objective Optimization of Exergetic Efficiency.

Based on the data presented in Figs.11 and 12, it can be observed that the findings suggest an optimized target for the payback period lies within the range of 4 to 13 years. Additionally, the exergy range is projected to be between 13 to 33 percent, respectively.

To simplify the outcomes of multi-objective optimization, one can refer to Fig.11 for a visual representation. By examining Fig.11, it becomes possible to easily calculate the exergy efficiency and payback period in relation to each other.

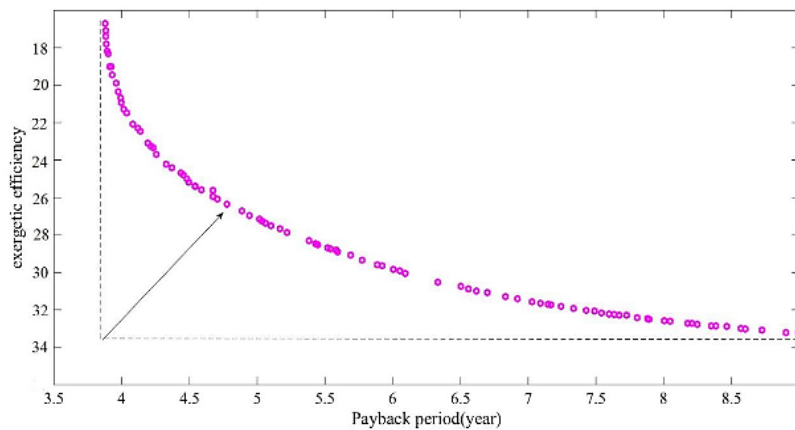


Fig. 11. Results of optimization for exergy efficiency vs. Payback period.

An analysis was conducted on the impact of various parameters, including the rate of biomass consumption, crude milk consumption rate, PVT surface area, the temperature of the combustion chamber, the cooling capacity of the absorption cycle, and turbine inlet pressure, on both the payback period and exergy efficiency.

Figure 12 illustrates that as the consumption rate of biomass rises, the exergy efficiency will decline. Conversely, reducing the consumption

rate of crude milk will also lead to a decrease in efficiency, owing to a lower production rate within the cycle.

As indicated in Fig. 13, the surface area of PVT panels has a negligible effect on the efficiency and payback period of the cycle. This is primarily because the overall efficiency of PVT panels surpasses that of biomass systems, thereby making any changes in the biomass system more apparent

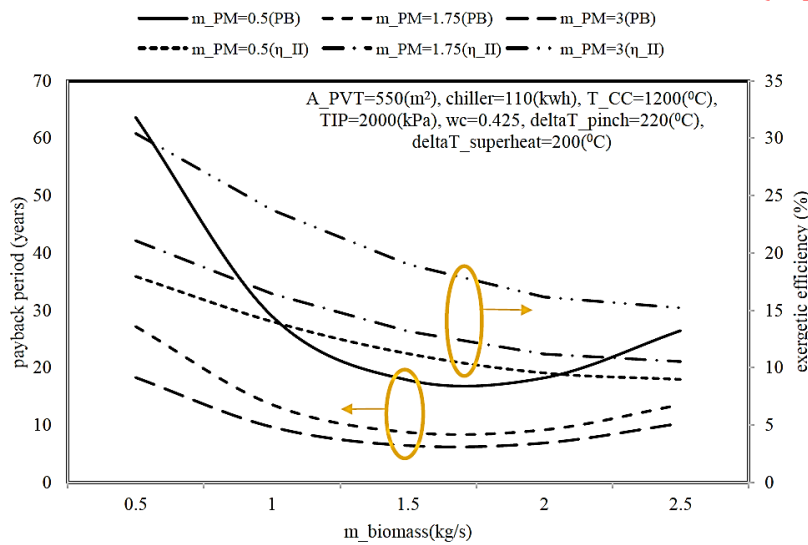


Fig. 12. Impact Of Biomass Consumption And Crude Milk Consumption Rate On Payback Period And Exergy Efficiency.

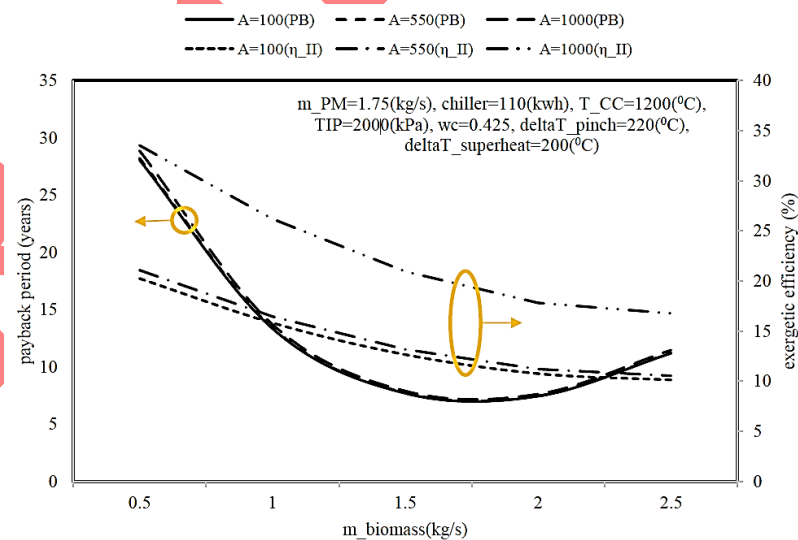


Fig.13. Impact Of Biomass Consumption And Pvt Surface Area Rate On Payback Period And Exergy Efficiency

Increasing the cooling capacity of the absorption cycle, as depicted in Fig. 14, clearly results in a longer payback period. This highlights the significant expenses associated with producing cooling capacity in the absorption cycle.

Figure 15 illustrates that elevating the temperature within the combustion chamber leads to a slight reduction in the payback period. Moreover, augmenting the temperature enhances

the exergy efficiency; however, it concurrently results in increased costs for the combustion chamber due to the utilization of more advanced technological construction techniques.

By contrasting Figs. 15 and 16, it becomes apparent that the impact of combustion chamber temperature surpasses that of turbine inlet pressure when considering exergy efficiency. Conversely, the turbine inlet pressure exhibits a greater influence on the payback period.

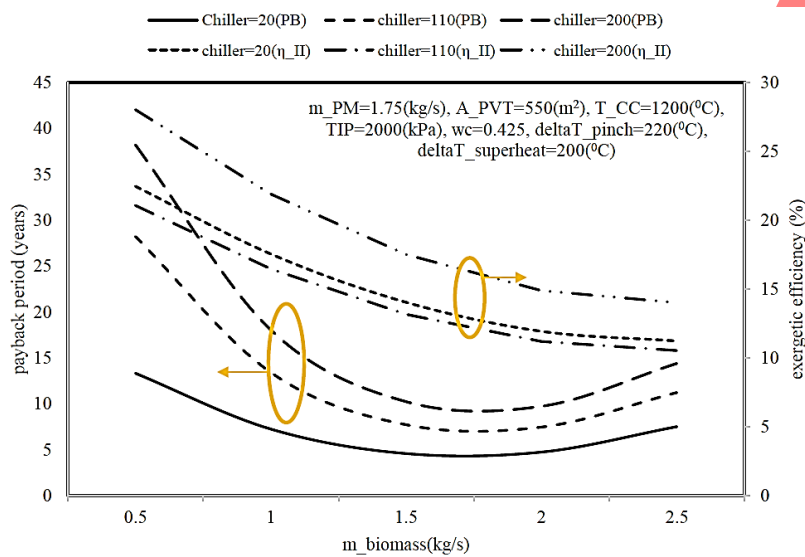


Fig. 14. Impact Of Biomass Consumption And Absorption Cycle Cooling Capacity On Payback Period And Exergy Efficiency.

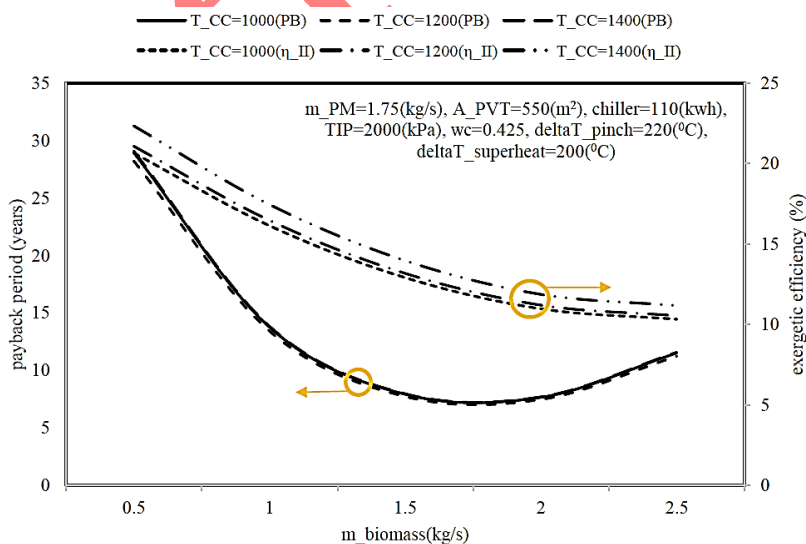


Fig. 15. Impact Of Biomass Consumption And Combustion Chamber Temperature On Payback Period And Exergy Efficiency.

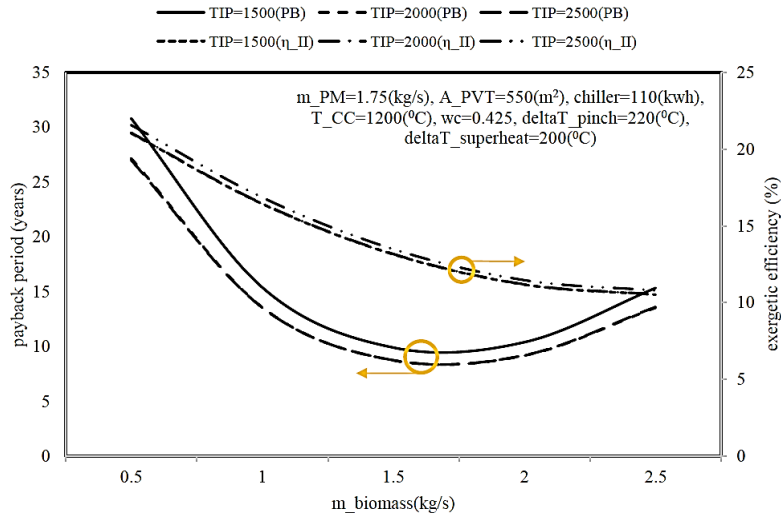


Fig. 16. Impact Of Biomass Consumption And Turbine Inlet Pressure On Payback Period And Exergetic Efficiency

Table 4 Exergy destruction rate equation for each component

Component	Exergy Destruction	Component	Exergy Destruction
Anaerobic Digester	$\dot{E}_{D,Dig} = \dot{E}_5 + \dot{E}_6 - \dot{E}_7 - \dot{E}_{8a}$	Expansion Valve 2	$\dot{E}_{D,exv2} = \dot{E}_{24} - \dot{E}_{25}$
Combustion Chamber	$\dot{E}_{D,cc} = \dot{E}_8 + \dot{E}_9 - \dot{E}_{10a}$	Absorption Cycle Pump	$\dot{E}_{D,PRef} = \dot{W}_{rp} - (\dot{E}_{21} - \dot{E}_{20})$
Combustion Gases Exhaust Fan	$\dot{E}_{D,ExF} = \dot{W}_{exf} - (\dot{E}_{11c} - \dot{E}_{11})$	PVT	$\dot{E}_{D,coll} = \dot{E}_{S,abs} - (\dot{E}_{31} + \dot{W}_{coll})$
Rankine Cycle Pump	$\dot{E}_{D,Pr} = \dot{W}_{Pr} - (\dot{E}_2 - \dot{E}_1)$	Pasteurizer	$\dot{E}_{D,pas} = (\dot{E}_{32} - \dot{E}_{33}) - (\dot{E}_{27} - \dot{E}_{26})$
Steam Turbine	$\dot{E}_{D,St} = \dot{E}_3 - \dot{E}_4 - \dot{W}_{st}$	Absorption Cycle Cooler	$\dot{E}_{D,coolRef} = (\dot{E}_{14} - \dot{E}_{15}) - (\dot{E}_{29} - \dot{E}_{28})$
Steam Generator	$\dot{E}_{D,sg} = \dot{E}_2 + \dot{E}_{10} - \dot{E}_3 - \dot{E}_{11a}$	Dryer Evaporator	$\dot{E}_{D,EvaPM} = (\dot{E}_{30a} - \dot{E}_{30b}) - (\dot{E}_{42} - \dot{E}_{27}) - \dot{E}_{30c}$
Rankine Condenser	$\dot{E}_{D,CondR} = \dot{E}_{12} + \dot{E}_4 - \dot{E}_1 - \dot{E}_{13}$	Dryer Pump	$\dot{E}_{D,PPM} = (\dot{E}_{43} - \dot{E}_{42}) - \dot{W}_{PPM}$
Absorption Cycle Generator	$\dot{E}_{D,GRef} = \dot{E}_{22} - \dot{E}_{16} - \dot{E}_{23} + \dot{E}_{34} - \dot{E}_{35}$	Dryer Cooler	$\dot{E}_{D,CoolPM} = (\dot{E}_{45} - \dot{E}_{44}) - (\dot{E}_{47} - \dot{E}_{46})$
Absorption Cycle Condenser	$\dot{E}_{D,ConRef} = \dot{E}_{16} + \dot{E}_{38} - \dot{E}_{39} - \dot{E}_{17}$	Dryer Economizer	$\dot{E}_{D,eco} = (\dot{E}_{55} - \dot{E}_{54}) - (\dot{E}_{48} - \dot{E}_{47})$
Absorption Cycle Evaporator	$\dot{E}_{D,EvaRef} = \dot{E}_{18} + \dot{E}_{36} - \dot{E}_{19} - \dot{E}_{37}$	Dryer Fan	$\dot{E}_{D,fanPM} = \dot{W}_{fanPM} - (\dot{E}_{49} - \dot{E}_{48})$
Absorption Cycle Absorber	$\dot{E}_{D,absRef} = \dot{E}_{19} + \dot{E}_{40} + \dot{E}_{25} - \dot{E}_{20} - \dot{E}_{41}$	Dryer Heater	$\dot{E}_{D,heat} = \dot{E}_{50a} - \dot{E}_{50b} - (\dot{E}_{50} - \dot{E}_{49} + \dot{E}_{50c})$
Absorption Cycle heat Exchanger	$\dot{E}_{D,ExRef} = \dot{E}_{21} - \dot{E}_{22} + \dot{E}_{23} - \dot{E}_{24}$	Dryer Compressor	$\dot{E}_{D,comp} = \dot{W}_{comp} - (\dot{E}_{53} - \dot{E}_{52})$
Expansion Valve 1	$\dot{E}_{D,exv1} = \dot{E}_{18} - \dot{E}_{17}$	Dryer	$\dot{E}_{D,drier} = (\dot{E}_{53} + \dot{E}_{51} - \dot{E}_{54}) - (\dot{E}_{44} - \dot{E}_{43})$

Table 5 Exergy-Economic Equation for each component

Component	Exergy-Economic Equation	Component	Exergy-Economic Equation
Anaerobic Digestor	$\dot{C}_7 + \dot{Z}_{Dig} = \dot{C}_8$	Absorption Cycle Absorber	$\dot{C}_{18} + \dot{C}_{15} + \dot{Z}_{EvaRef} = \dot{C}_{20} + \dot{C}_{41}, c_{25} = c_{20}, c_{40} = c_{41}$
Combustion Chamber	$\dot{C}_8 + \dot{C}_9 + \dot{Z}_{CC} = \dot{C}_{10}$	Absorption Cycle Evaporator	$\dot{C}_{14} + \dot{C}_{28} + \dot{Z}_{coolRef} = \dot{C}_{15} + \dot{C}_{29}, c_{14} = c_{15}, c_{28} = c_{29}$
Rankine Cycle Pump	$\dot{C}_1 + \dot{Z}_{Pr} + \dot{C}_{W,Pr} = \dot{C}_2, c_{W,Pr} = c_{W,St}, c_1 = c_2$	PVT	$\dot{Z}_{Sol} = \dot{C}_{31} + \dot{W}_{sol}, c_{w,Sol} = c_{w,Pr}$
Steam Turbine	$\dot{C}_3 + \dot{Z}_{St} = \dot{C}_{W,St} + \dot{C}_4, c_4 = c_3$	Pasteurizer	$\dot{C}_{32} + \dot{C}_{26} + \dot{Z}_{pas} = \dot{C}_{33} + \dot{C}_{27}, c_{32} = c_{33}, c_{26} = c_{27}$
Steam Generator	$\dot{C}_2 + \dot{C}_{10} + \dot{Z}_{Sg} = \dot{C}_{11} + \dot{C}_3, c_{11} = c_{10}$	Dryer Evaporator	$\dot{C}_{27} + \dot{C}_{30a} + \dot{Z}_{EvaPM} = \dot{C}_{30c} + \dot{C}_{30b} + \dot{C}_{42}, c_{30a} = c_{30c}, c_{27} = c_{42}$
Rankine Condenser	$\dot{C}_4 + \dot{C}_{12} + \dot{Z}_{CondR} = \dot{C}_{13} + \dot{C}_1, c_4 = c_1$	Milk Powder Pump	$\dot{C}_{42} + \dot{Z}_{PPM} + \dot{C}_{w,PPM} = \dot{C}_{43}, c_{42} = c_{43}, c_{w,PPM} = c_{w,Pr}$
Exhaust Fan	$\dot{C}_{48} + \dot{Z}_{ExF} + \dot{C}_{W,ExF} = \dot{C}_{49}, c_{W,ExF} = c_{w,Pr}, c_{48} = c_{49}$	Dryer Economizer	$\dot{C}_{47} + \dot{C}_{54} + \dot{Z}_{eco} = \dot{C}_{48} + \dot{C}_{55}, c_{47} = c_{48}, c_{54} = c_{55}$
Absorption Cycle Generator	$\dot{C}_{22} + \dot{C}_{34} + \dot{Z}_{GRef} = \dot{C}_{16} + \dot{C}_{23} + \dot{C}_{35}, c_{34} = c_{35}$	Dryer Fan	$\dot{C}_{48} + \dot{Z}_{fanPM} + \dot{C}_{w,fanPM} = \dot{C}_{49}, c_{48} = c_{49}, c_{w,fanPM} = c_{w,Pr}$
Absorption Cycle Condenser	$\dot{C}_{16} + \dot{C}_{38} + \dot{Z}_{conRef} = \dot{C}_{17} + \dot{C}_{39}, c_{16} = c_{17}, c_{38} = c_{39}$	Dryer Compressor	$\dot{C}_{52} + \dot{Z}_{comp} + \dot{C}_{w,comp} = \dot{C}_{53}, c_{52} = c_{53}, c_{w,comp} = c_{w,Pr}$
Absorption Cycle Heat Exchanger	$\dot{C}_{21} + \dot{C}_{23} + \dot{Z}_{ExRef} = \dot{C}_{22} + \dot{C}_{24}, c_{21} = c_{22}, c_{23} = c_{24}$	Dryer Heater	$\dot{C}_{49} + \dot{C}_{50a} + \dot{Z}_{heat} = \dot{C}_{50} + \dot{C}_{50b} + \dot{C}_{50c}, c_{50a} = c_{50b}$
Absorption Cycle Pump	$\dot{C}_{21} + \dot{Z}_{PRef} + \dot{C}_{w,pRef} = \dot{C}_{22}, c_{21} = c_{22}, c_{w,pRef} = c_{w,Pr}$	Dryer Fan	$\dot{C}_{53} + \dot{C}_{43} + \dot{C}_{51} + \dot{Z}_{drier} = \dot{C}_{44} + \dot{C}_{54}$
Absorption Cycle Absorber	$\dot{C}_{19} + \dot{C}_{25} + \dot{C}_{40} + \dot{Z}_{absRef} = \dot{C}_{20} + \dot{C}_{41}, c_{25} = c_{20}, c_{40} = c_{41}$	Dryer Cooler	$\dot{C}_{46} + \dot{C}_{44} + \dot{Z}_{coolPM} = \dot{C}_{47} + \dot{C}_{45}, c_{44} = c_{45}, c_{46} = c_{47}$

Table 6 Exergy-Economic Equation for each component

Component	Exergy-Economic Equation	Exergy-Economic Equation
Anaerobic Digestor	$\dot{C}_7 + \dot{Z}_{Dig} = \dot{C}_8$	$\dot{C}_{18} + \dot{C}_{15} + \dot{Z}_{EvaRef} = \dot{C}_{20} + \dot{C}_{41}, c_{25} = c_{20}, c_{40} = c_{41}$
Combustion Chamber	$\dot{C}_8 + \dot{C}_9 + \dot{Z}_{CC} = \dot{C}_{10}$	$\dot{C}_{14} + \dot{C}_{28} + \dot{Z}_{coolRef} = \dot{C}_{15} + \dot{C}_{29}, c_{14} = c_{15}, c_{28} = c_{29}$
Anaerobic Digestor	$\dot{C}_7 + \dot{Z}_{Dig} = \dot{C}_8$	$\dot{C}_{18} + \dot{C}_{15} + \dot{Z}_{EvaRef} = \dot{C}_{20} + \dot{C}_{41}, c_{25} = c_{20}, c_{40} = c_{41}$
Combustion Chamber	$\dot{C}_8 + \dot{C}_9 + \dot{Z}_{CC} = \dot{C}_{10}$	$\dot{C}_{14} + \dot{C}_{28} + \dot{Z}_{coolRef} = \dot{C}_{15} + \dot{C}_{29}, c_{14} = c_{15}, c_{28} = c_{29}$
Anaerobic Digestor	$\dot{C}_7 + \dot{Z}_{Dig} = \dot{C}_8$	$\dot{C}_{18} + \dot{C}_{15} + \dot{Z}_{EvaRef} = \dot{C}_{20} + \dot{C}_{41}, c_{25} = c_{20}, c_{40} = c_{41}$
Combustion Chamber	$\dot{C}_8 + \dot{C}_9 + \dot{Z}_{CC} = \dot{C}_{10}$	$\dot{C}_{14} + \dot{C}_{28} + \dot{Z}_{coolRef} = \dot{C}_{15} + \dot{C}_{29}, c_{14} = c_{15}, c_{28} = c_{29}$
Anaerobic Digestor	$\dot{C}_7 + \dot{Z}_{Dig} = \dot{C}_8$	$\dot{C}_{18} + \dot{C}_{15} + \dot{Z}_{EvaRef} = \dot{C}_{20} + \dot{C}_{41}, c_{25} = c_{20}, c_{40} = c_{41}$
Combustion Chamber	$\dot{C}_8 + \dot{C}_9 + \dot{Z}_{CC} = \dot{C}_{10}$	$\dot{C}_{14} + \dot{C}_{28} + \dot{Z}_{coolRef} = \dot{C}_{15} + \dot{C}_{29}, c_{14} = c_{15}, c_{28} = c_{29}$
Anaerobic Digestor	$\dot{C}_7 + \dot{Z}_{Dig} = \dot{C}_8$	$\dot{C}_{18} + \dot{C}_{15} + \dot{Z}_{EvaRef} = \dot{C}_{20} + \dot{C}_{41}, c_{25} = c_{20}, c_{40} = c_{41}$
Combustion Chamber	$\dot{C}_8 + \dot{C}_9 + \dot{Z}_{CC} = \dot{C}_{10}$	$\dot{C}_{14} + \dot{C}_{28} + \dot{Z}_{coolRef} = \dot{C}_{15} + \dot{C}_{29}, c_{14} = c_{15}, c_{28} = c_{29}$

Table 7. Capital cost Equation for each component of the cycle [13,12]

Component	Capital Cost Estimation	Remarks
Anaerobic Digester	$Z_{Dig} = 35000 \left(\frac{VT}{21000} \right)^{0.75}$	V : Volumetric Flow Rate T : Working Temperature
Combustion Chamber	$Z_{cc} = c_1 \dot{m}_{air} (1 + \exp(c_2 T_{out} - c_3)) \dots$ $\frac{1}{0.995 - \frac{P_{out}}{P_{in}}}$, $c_1 = 48.64\$ / (kg / s)$ $c_2 = 0.018K^{-1}$, $c_3 = 26.4$	T_{out} : Outlet Temperature of Combustion Chamber $\frac{P_{out}}{P_{in}}$: pressure ratio of Combustion Chamber
Rankine Cycle Pump	$Z_{PR} = c_4 (\dot{W}_{Pr})^{0.71}$, $c_4 = 3540\$ / (kW)^{0.71}$	\dot{W}_{Pr} : Pump Brake Horse Power
Steam Turbine	$Z_{ST} = c_5 (\dot{W}_{St})^{0.7}$, $c_5 = 6000\$ / (kW)^{0.7}$	\dot{W}_{St} : Turbine Output Power
Steam Generator	$Z_{SG} = 6570 \left(\left(\frac{\dot{Q}_{ec}}{\Delta T_{m,ec}} \right)^{0.8} + \left(\frac{\dot{Q}_{ev}}{\Delta T_{m,ev}} \right)^{0.8} \right) \dots$ $+ 21276 \dot{m}_g + 1184.4 \dot{m}_g^{1.2}$	$\Delta T_{m,ec}$: Temperature Difference of inlet and outlet Gas $\Delta T_{m,ev}$: Temperature Difference of water inlet and steam outlet Q_{ec} : Gas Heat transfer Q_{ev} : Steam heat Transfer \dot{m}_s : Steam mas flow Rate \dot{m}_g : Gas Mass flow Rate
Rankine Condenser	$Z_{CondR} = c_9 \dot{m}_{water}$, $c_9 = 1773\$ / (kg / s)$	\dot{m}_{water} : Water mass Flow rate
Exhaust Fan	$Z_{ExF} = 2833 (\dot{m}_{exG})^{0.7053}$	\dot{m}_{exG} : Exhaust Gas Mass Flow rate
Absorption Cycle Generator	$Z_{GRef} = 17500 \left(\frac{A_{gen}}{100} \right)^{0.06}$	A_{gen} : Surface Area of Generator
Absorption Cycle Condenser	$Z_{CondRef} = c_9 \dot{m}_{water}$, $c_9 = 1773\$ / (kg / s)$	\dot{m}_{water} : Water mass Flow Rate
Absorption Cycle Heat Exchanger	$Z_{ExRef} = 4760 A_{ex}^{0.68}$	A_{ex} : Surface Area of Heat Exchanger
Absorption Cycle Pump	$Z_{PRef} = c_4 (\dot{W}_{PRef})^{0.71}$ $c_4 = 3540\$ / (kW)^{0.71}$	\dot{W}_{PRef} : Pump Brake Horse Power
Absorption Cycle Absorber	$Z_{AbsRef} = 16000 \left(\frac{A_{abs}}{100} \right)^{0.06}$	A_{abs} : Surface Area of Absorber
Absorption Cycle Evaporator	$Z_{EvaRef} = 16000 \left(\frac{A_{ev}}{100} \right)^{0.06}$	A_{ev} : Surface Area of Evaporator
Absorption Cycle Cooler	$Z_{coolRef} = 4760 A_{cool}^{0.68}$	A_{cool} : Surface Area of Cooler
PVT	$Z_{PVT} = 310 A_{PVT}$	A_{PVT} : Surface Area of PVT Exposed to Sun
Pasteurizer	$Z_{Pas} = 4680 (A_{pas})^{0.742}$	A_{pas} : Surface Area of Pasturized
Milk Powder Cycle Evaporator	$Z_{EvaPM} = 51733 \ln(A_{evaPM}) - 74437$	A_{evaPM} : Surface Area of Evaporator
Milk Powder Cycle Pump	$Z_{PPM} = 5870 (\dot{W}_{PPP})^{0.85}$	\dot{W}_{PPP} : Pump Brake Horse Power
Milk Powder Cycle Economizer	$Z_{eco} = 1644 A_{eco}^{0.81} + 18900$	A_{eco} : Surface Area of Economizer
Milk Powder Cycle Blower	$Z_{fanPM} = 2833 (\dot{m}_{airPM})^{0.7053}$	\dot{m}_{airPM} : Mass Flow Rate of Air
Compressor	$Z_{AC} = \left(\frac{c_{10} \dot{m}_{air}}{c_{11} - \eta_{is,AC}} \right) \left(\frac{P_{out}}{P_{in}} \right) \ln \left(\frac{P_{out}}{P_{in}} \right)$ $c_{10} = 75 / (kg / s)$, $c_{11} = 0.9$	\dot{m}_{air} : Mass Flow Rate of Air $\frac{P_{out}}{P_{in}}$: Compressor Pressure Ratio
Milk Powder Cycle Heater	$Z_{heat} = 1644 A_{heat}^{0.81} + 18900$	A_{heat} : Surface Area of Heater
Milk Powder Cycle Dryer	$Z_{drier} = 35800 (\dot{m}_{pm})^{0.3048}$	\dot{m}_{pm} : Mass Flow Rate of Milk Powder
Milk Powder Cycle Cooler	$Z_{coolPM} = 5430 A_{coolPM}^{0.7}$	A_{coolPM} : Surface Area of Cooler

4. Conclusions

In this study, the objective was to enhance the performance of the Combined Cooling, Heating, and Power (CCHP) cycle by considering the payback period and exergy efficiency. Initially, each component of the cycle was verified by comparing it with relevant literature, and the outcomes of this validation process were presented. The paper also presents the results of multi-objective optimization. When focusing solely on minimizing the payback period, the cycle can be configured to achieve a minimum payback period of 3.82 years. On the other hand, if the goal is to maximize system efficiency, the system can be adjusted to reach a maximum efficiency of 24.7. In cases where both efficiency and a short payback period are desired. The multi-objective optimization results indicate that a system with an optimized efficiency of 27 percent will have a payback period of 4.8 years. Also, the effect of several performance parameters of the cycle of exergy efficiency and payback period has been studied. Results indicate that the most impact is caused by the biomass consumption rate due to the lower efficiency of this system compared to other components. Another parameter is turbine inlet pressure which has a massive impact on payback period and little impact on exergy efficiency. Also, as the cooling capacity of the cycle increases the payback period is due to the fact that the cost of cooling capacity produced by the absorption cycle is high.

In the present work, biomass was utilized for powering the cycle. In future works, the effect of utilizing other renewable energy sources such as wind or solar can be studied. As stated earlier the aim of the present work is to minimize the cost of the cooling cycle which can be achieved by optimizing the refrigeration cycle or utilizing more advanced refrigeration technologies. The current study shows that the cost of the cooling cycle is relatively high which needs to be alleviated.

Acknowledgments

This research was supported by Iranian Fuel Conservation Company (IFCO). Authors appreciate colleagues of research and

development as well as energy optimization in building departments who provided insight and expertise that assisted the research.

References

- [1] Musharavati F, Khoshnevisan A, Alirahmi SM, Ahmadi P, Khanmohammadi S. Multi-objective optimization of a biomass gasification to generate electricity and desalinated water using Grey Wolf Optimizer and artificial neural network. *Chemosphere*. 2022;287:131980.
- [2] Rezvan AT, Gharneh NS, Gharehpetian G. Robust optimization of distributed generation investment in buildings. *Energy*. 2012;48(1):455-63.
- [3] Chlipała M, Błaszczak P, Wang S-F, Jasiński P, Bochentyn B. In situ study of a composition of outlet gases from biogas fuelled Solid Oxide Fuel Cell performed by the Fourier Transform Infrared Spectroscopy. *International Journal of Hydrogen Energy*. 2019;44(26):13864-74.
- [4] Worawimut C, Vivanpatarakij S, Watanapa A, Wiyaratn W, Assabumrungrat S. Performance evaluation of biogas upgrading systems from swine farm to biomethane production for renewable hydrogen source. *International Journal of Hydrogen Energy*. 2019;44(41):23135-48.
- [5] Abdeshahian P, Lim JS, Ho WS, Hashim H, Lee CT. Potential of biogas production from farm animal waste in Malaysia. *Renewable and Sustainable Energy Reviews*. 2016;60:714-23.
- [6] Pantaleo AM, Camporeale SM, Miliozzi A, Russo V, Shah N, Markides CN. Novel hybrid CSP-biomass CHP for flexible generation: Thermo-economic analysis and profitability assessment. *Applied energy*. 2017;204:994-1006.
- [7] Gürlich D, Dalibard A, Eicker U. Photovoltaic-thermal hybrid collector performance for direct trigeneration in a European building retrofit case study. *Energy and Buildings*. 2017;152:701-17.
- [8] Buswell AM. Anaerobic fermentations. *Bulletin (Illinois State Water Survey) no 32*. 1939.
- [9] Joshi A, Tiwari A, Tiwari G, Dincer I, Reddy B. Performance evaluation of a hybrid

- photovoltaic thermal (PV/T)(glass-to-glass) system. *International Journal of Thermal Sciences*. 2009;48(1):154-64.
- [10] Dincer I, Rosen MA, Ahmadi P. *Optimization of energy systems*: John Wiley & Sons; 2017.
- [11] Bejan A, Tsatsaronis G, Moran MJ. *Thermal design and optimization*: John Wiley & Sons; 1995.
- [12] Behzadi A, Houshfar E, Gholamian E, Ashjaee M, Habibollahzade A. Multi-criteria optimization and comparative performance analysis of a power plant fed by municipal solid waste using a gasifier or digester. *Energy Conversion and Management*. 2018;171:863-78.
- [13] Soltani S, Mahmoudi S, Yari M, Morosuk T, Rosen M, Zare V. A comparative exergoeconomic analysis of two biomass and co-firing combined power plants. *Energy Conversion and Management*. 2013;76:83-91.
- [14] Wellinger A, Murphy JP, Baxter D. *The biogas handbook: science, production and applications*: Elsevier; 2013.
- [15] Aman J, Ting D-K, Henshaw P. Residential solar air conditioning: Energy and exergy analyses of an ammonia–water absorption cooling system. *Applied Thermal Engineering*. 2014;62(2):424-32.
- [16] Yildirim N, Genc S. Energy and exergy analysis of a milk powder production system. *Energy Conversion and Management*. 2017;149:698-705.
- [17] Calise F, d'Accadia MD, Piacentino A. Exergetic and exergoeconomic analysis of a renewable polygeneration system and viability study for small isolated communities. *Energy*. 2015;92:290-307.
- [18] Wang J, Han Z, Guan Z. Hybrid solar-assisted combined cooling, heating, and power systems: A review. *Renewable and Sustainable Energy Reviews*. 2020;133:110256.

Retraction